International Journal of Applied Engineering & Technology

METHODOLOGY FOR CALCULATION OF VELOCITY AND DISPLACEMENT FOR BROAD FREQUENCY ACCELERATIONS USING FOURIER TRANSFORM AND NUMERICAL INTEGRATION

Alexandre James Gordon
One Subsea, agordon5@slb.com

Abstract - *The following paper gives a methodology for integration of acceleration to velocity and displacement for a broad range frequency spectrum. It shows how to avoid group delay, phase delay, minimise edge effects and remove low frequency noise in displacement data, utilising the advantages of omega arithmetic for high frequency data and numerical integration for low frequency data. Along with a process for how to split and re-combine the low and high frequencies to give a full spectrum of velocity and displacement data. Using the methodology described in this paper allows the use of the full capability of an accelerometer's measurement spectrum, resulting in a frequency range for the displacement data which was previously the realm of sensor fusion techniques (<0.001fs to Nyquist Frequency). To demonstrate the methodology described two sets of data are processed, a series of sinusoidal waves with frequencies from 0.5 to 400Hz and MEMS accelerometer data captured was compared to an infrared sensor with recorded frequencies from 0.03Hz to 20Hz.*

Index Terms – Integration, Calculus, Omega Arithmetic, MEMS, Accelerometer, Displacement, Velocity.

INTRODUCTION

In the field of engineering there are many occasions where acceleration data needs to be converted via integration to velocity and/or displacement. The number instances of this have now increased dramatically with adoption of MEMS (Micro-electromechanical systems) accelerometers in virtually every smart phone and piece of wearable technology. Despite this abundance of accelerometers, which are often used exclusively for calculation of velocity and displacement, there seems to be little guidance on how to approach the processing of broad frequency spectrum acceleration data, which is the norm for captured data. To add to this, there has been little which consolidates what the common issues are with integration of acceleration data and how to avoid them.

There has been research into the available techniques for integration routines for calculating acceleration to displacement. Much of the research to date has been focused on the limitations of each method, and comparative errors of those methods [4], [5] and [8]. Those studies that have been focused on a methodology, have eliminated the limitations of the frequency range for a particular integration method through filtering, this results in a narrow band of acceleration frequencies being integrated [9], [10] and [11], typically from $>0.01f_{max}$ to f_{max}. In all cases, as they have been performed with causal data, this has resulted in group delay. Other research has tried to address how to measure broad frequency data for displacements <0.001fs to Nyquist Frequency. In these cases, the data captured has been from multiple sensor types. Typically, an accelerometer for high frequency measurement ($>0.1f_s$) and another sensor type for low frequency displacement ($<0.1f_s$), using sensor fusion techniques to overcome the integration, or perceived instrument shortfalls at lower frequencies [12], [13], [14] and [15].

Although the research has been developed with a view to utilisation on specific equipment, its application is broad. It can be used where sensor fusion techniques have been used in the past, or in situations where the use of multiple sensors are not physically or economically feasible, but there is a need to capture and process both low and high frequency data.

THEORY

I. Numerical Integration

The most widely implemented methods for integration of data sets is numerical integration. There are multiple numerical integration types, but this paper will focus on Simpson's 3/8 rule, as it was found to be the most accurate for the data set used.

Simpson's 3/8 rule is given by [1]:

$$\int_a^b f(x) \approx \frac{b-a}{8}\left[f(a) + 3f\left(\frac{2a+b}{3}\right) + 3f\left(\frac{a+2b}{3}\right) + f(b)\right]$$

The error bound for Simpson's 3/8 rule is [1]:

$$\left|E_{3/8}\right| \leq \frac{3(b-a)^5}{80N^5}\left[max\left|f^{(4)}(x)\right|\right]$$

Something to note from the error formulae is that regardless of the sample rate and duration, numerical integration will always suffer from some level of error. When performing double integration, from acceleration to displacement, the velocity error is also integrated, causing the displacement to drift. This can be corrected by removing the velocity offset and displacement drift by using a linear regression [2].

$$m = \frac{N\sum(xy) - \sum x \sum y}{N\sum x^2 - (\sum x)^2}$$

$$c = \frac{\sum y - m\sum x}{N}$$

II. Fourier Transform and Omega Arithmetic

As the displacement drift and velocity offset inherent to numerical integration are amplified by acceleration data with high frequencies/rapid changes, a more suitable method must be found if high rates of change are present. This is where the Fourier Transform can help [7]:

$$X(k) = \sum_{n=0}^{N-1} x(n) e^{\frac{-2\pi i k n}{N}}$$

Omega arithmetic uses the data in the frequency domain to integrate exactly. This is performed by converting a data set to the frequency domain using the DFT (Discrete Fourier Transform) or FFT (Fast Fourier Transform) and multiplying the data by the frequency response function. For a single integration the function would be:

$$H(f) = \frac{1}{2\pi i f}$$

To simplify the above, 2πf is often denoted as ω, hence, Omega Arithmetic. However, this method of integration does have a limitation, that is when the data gets to low frequencies, approximately 0.001fs then the results tend to infinity.

To avoid this issue a high pass filter can be used to remove all low frequency data and the omega arithmetic can be performed.

III. Fourier Transform Filtering and Phase/Group Delay

During the previous sections, it has been shown that numerical integration, such as Simpson's rule, is suitable for low frequency data, and Omega Arithmetic is suitable for high frequency data. Combining these two integration methods would then allow broad frequency spectrum acceleration data to be processed, from about 0.0001fs to the Nyquist frequency for a particular sample rate.

To be able to use different methods of integration together, the data needs to be filtered to allow for different frequency ranges to be processed separately. High frequency data can use Omega arithmetic, which is accurate to 0.001fs. Numerical integration errors are dependent on the sample number and frequency, but a good starting point is 0.01fs for upper bound frequencies.

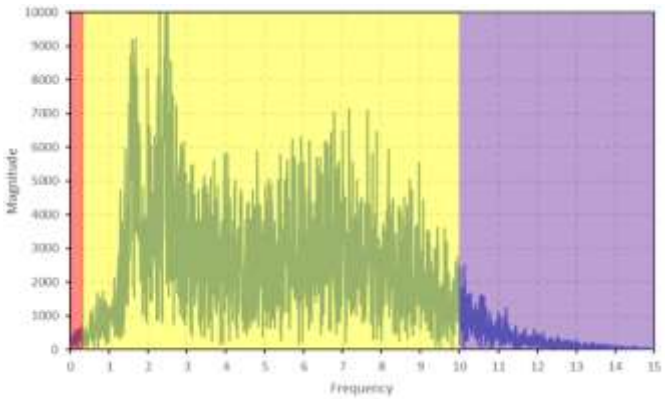

FIGURE 1

CHART SHOWING FREQUENCY SPLIT BETWEEN THE INTEGRATION METHODS. THE RED SECTION IS LOW FREQUENCY DATA THAT IS FILTERED OUT. THE YELLOW SECTION IS THE LOW FREQUENCY DATA WHICH USES NUMERICAL INTEGRATION. THE PURPLE SECTION IS THE HIGH FREQUENCY DATA WHICH USES OMEGA ARITHMETIC UP TO THE NYQUIST FREQUENCY.

In broad terms, there are two different ways to filter data, infinite impulse response filters (IIR) and finite impulse response filters (FIR). As this paper is using non-causal data, it will focus on IIR filtering. The issues that can affect the data once filtered are:

Phase Delay: Different parts of the frequency spectrum get moved in the time domain when the filter has been applied and it is converted back to the time domain. The effect is stronger over frequencies where the filter is ramping up or down. IIR filters suffer from phase delay, FIR do not.

Group Delay: This is the delay of all frequencies when a filter has been applied and they are converted back to the time domain. Both IIR and FIR filters suffer from group delay.

Both the phase and group delay when using an IIR filter can be corrected by filtering the data with time running forwards, then reversing time and re-filtering the data. Effectively moving the delay forwards, then backwards to remove it.

Step 1:

$$x_{(0,1,2\ldots n)}(t) \xrightarrow[FFT]{} X(f) \cdot F(f) \xrightarrow[IFFT]{} x'_{(0,1,2\ldots n)}(t)$$

Step 2:

$$x'_{(n,n-1,n-2\ldots 0,1)}(t) \xrightarrow[FFT]{} X(f) \cdot F(f) \xrightarrow[IFFT]{} x''_{(n.n-1,n-2\ldots 0,1)}(t)$$

There are several different types of IIR filters, but this routine will use the Butterworth filter [3].

$$F(f) = \frac{1}{\sqrt{1 + \left(\frac{f}{f_{cutoff}}\right)^{2p}}}$$

IV. Edge Cases

In all cases the captured acceleration data will be a finite length. To address this the Fast Fourier Transform assumes that the beginning of the data is joined to the end of the data series, creating a loop of data. If there are large differences between the final points of the data series and the initial points of the data series, then this can cause edge effects.

This is best addressed by using reflection, where the data is reflected at the beginning and end of the data set. Consider the array below:

n_1	n_2	n_2	n_3	n_4	n_5
1	2	3	4	5	6

This would then be reflected to give an array twice the size which would be:

n_1	n_2	n_3	n_4	n_5	n_6	n_7	n_8	n_9	n_{10}	n_{11}	n_{12}
4	3	2	1	2	3	4	5	6	5	4	3

The doubling in size is to allow for a common property of the FFT that they are typically of size 2^n. It should be noted that doing this doubles the size of the processing required.

V. Additional Filtering of Displacement Data

For data where there are large amplitude high frequency accelerations, there is often noise which results in a characteristic parabolic displacement output. This is caused by low frequency noise, that has a frequency that is half the period of the total data set length, generated from the high frequency components.

To address this, the displacement data can be re-filtered using the same method as the high pass filter that was used on the acceleration data. This step is not necessarily required, it is only a requirement where there are strong high frequency components, which result in a parabolic output.

VI. Methodology for Calculation of Velocity and Displacement of Broad Frequency Accelerations

Considering the previous sections, a flow chart for the processing of data can be made to allow for broad frequency integration to be done.

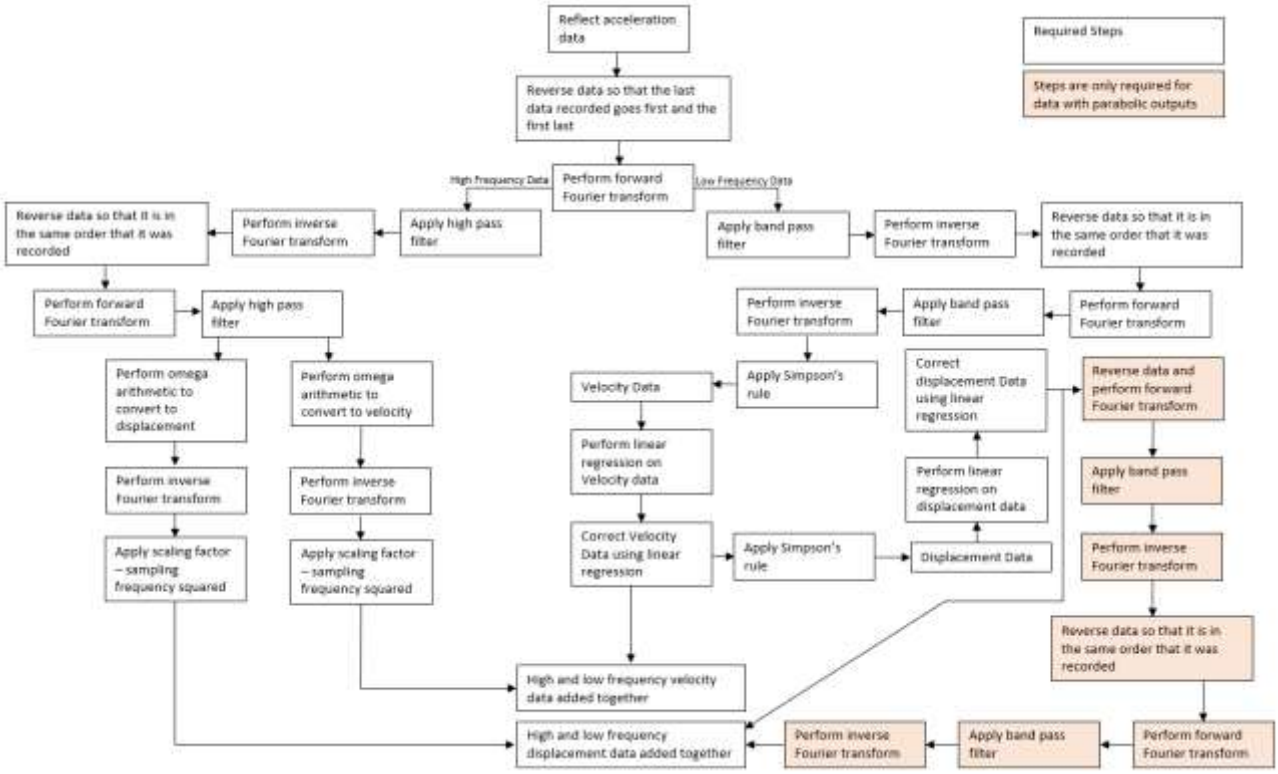

FIGURE II FLOW CHART OF METHODOLOGY FOR CALCULATION OF VELOCITY AND DISPLACEMENT FOR BROAD FREQUENCY ACCELERATIONS

The Butterworth filter has a value of 0.707 at f_{cutoff}. This will give some slightly higher velocities/displacements around f_{cutoff} if the low and high frequency data are added together. This can be addressed by moving the cut off for the low pass and high pass filters so at f_{cutoff} they sum to 1. To identify the ideal cut off point the below can be used to solve for x which is the offset from the ideal cut off point on the data. Note: this identity is only for data which has been filtered forwards and backwards, resulting in the square of the Butterworth filter.

$$1 = \left\{\left[1 + \left(\frac{f_{cutoff} - x_{off}}{f_{cutoff}}\right)^{2p}\right]^{-0.5}\right\}^2 + \left\{\left[1 + \left(\frac{f_{cutoff}}{f_{cutoff} + x_{off}}\right)^{2p}\right]^{-0.5}\right\}^2$$

RESULTS

To test the methodology a series of sin waves were used all with varying amplitudes and a data rate of 1000Hz. The frequencies chosen were, 0.5Hz, 9Hz, 50Hz and 400Hz. The accelerations from these frequencies were summed and put through the routine. To be able to compare them they were integrated to find the corresponding velocity and displacement curves. The amplitudes chosen were, 1g for 0.5Hz, 8g for 9Hz, 250g for 50Hz and 16000g for 400Hz, these would allow all frequencies to be easily identifiable in the displacement output. After processing, there were some strong edge effects caused by the truncation of the signal at the end of the time series. Using the below for error calculation, the average error for the whole signal was 10.31%, however, if the edge effects are not considered the average error was 1.51%.

$$Error\% = 100\frac{\sqrt{{s_{calc}}^2 - {s_{actual}}^2}}{RMS_{actual}}$$

To check the routine against real data, a second test was performed using an accelerometer with a data rate of 1000Hz which was put onto a sprung and damped platform. The assembly was then moved with some long period and short period movements. This was checked against an infra-red (IR) range finder. The results of the IR data plotted against the calculated data are shown in Figure III. The two systems produced similar results with a 10.07% absolute difference across the captured data series. This difference was calculated using the below:

$$Difference\% = 100\frac{\sqrt{{s_{calc}}^2 - {s_{IR}}^2}}{RMS_{IR}}$$

DISCUSSION

For both the data sets run through the routine the output was close to the expected output. The difference between the IR data and the routine was due to the response time of the IR sensor which resulted in a stepping function and high frequency noise in the IR signal, which can be seen clearly in Figure III. For the sin curves the main issue was the edge effect which was emphasised due to the high amplitude of the high frequency components.

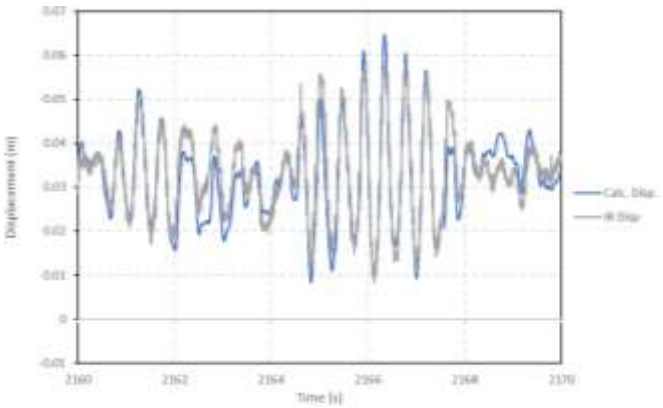

FIGURE III DISPLACEMENT OUTPUT FROM COMBINATION INTEGRATION ROUTINE FOR ACCELEROMETER DATA

Another finding was that for both data types, the low frequency high pass filter cut off and power needed to be tuned to give the best results. For the sin curves the best results found were when the cut off was set to 0.4Hz and the power was set to 11. For the data that was compared to the IR sensor the results were best when the cut off was set to 0.7Hz and the power was set to 0.55.

The additional filtering of the displacement output is not necessarily required. The IR data was identical with and without additional filtering of the displacement data. Conversely, the sin curves had to have the displacement data filtered to remove the characteristic parabolic shape. When the amplitude of the higher frequency components of the data were reduced, filtering the displacement data was not required.

CONCLUSION

The routine developed in this paper works well with different types of data over a broad spectrum of frequencies.

For applications where multiple sensor types cannot be utilised, or it is cost prohibitive, the work shown provides a novel methodology for using an accelerometer for displacement calculation, that will utilise all the instrument's full

range by eliminating the shortfalls of the integration and filtering methods allowing a measurement from <0.001fs to Nyquist Frequency. The research also provides some guidance on how to get the most from the methodology and how it can be modified to improve results further.

REFERENCES

[1] P. J. Davis and P. Rabinowitz, Methods of Numerical Integration, 2nd Edition, Academic Press, London (1984)
[2] M. Rouaud, Probability, Statistic and Estimation, Short Edition, (2013)
[3] L. D. Paarmann, Design and Analysis of Analog Filters, Kluwer Academic Publishers, New York (2001)
[4] A. Brandt, R. Brincker, Integrating time signals in frequency domain – Comparison with time domain integration, Measurement, 58 (2014)511-519
[5] S. Han, Measuring displacement signal with an accelerometer, Journal of Mechanical Science and Technology, 24 (6)(2010)1329-1335
[6] P. J. Davis, Interpolation and Approximation, Dover Publications, New York (1975)
[7] K.R. Rao, D.N. Kim, J.J. Hwang, Fast Fourier Transform: Algorithms and Applications, Springer (2010)
[8] R. Brincker, FFT Integration of Time Series using an Overlap-Add Technique, Proceedings of the IMAC-XXVIII, Jacksonville USA (2010)
[9] W. Zheng, D. Dan, W. Cheng, Y. Xia, Real-time dynamic displacement monitoring with double integration of acceleration based on recursive least squares method, Measurement, 141 (2019) 460-471
[10] H. Kanamori, P. Maechling, Continuous monitoring of ground-motion parameters, Bulletin of the Seismological Society of America, (1999) 89 (1): 311–316.
[11] C. Han, X. Hu, An Absolute Displacement Measurement Method and its Application in Ship Motion Measurement, Journal of Marine Science and Engineering, (2023) 11, 931
[12] S. Joh, Dynamic Deflection of a Railroad Sleeper from the Coupled Measurement of Acceleration and Strain, Sensors, 2018(7), pp. 2182–2182
[13] S. Yang, C. Xu, J. Mi, S. Gu, Dynamic Deformation Monitoring of Offshore Oil Platforms with Integrated GNSS and Accelerometers, Sustainability, (2022) 14 (10521): 10521–10521.
[14] J. Han, X. Yang, H. Li, H. Cui, Error Correction of Measured Unstructured Road Profiles Based on Accelerometer and Gyroscope Data, Mathematical Problems in Engineering, (2017) 2017 pp. 1-11
[15] Z. Ma, J. Choi, H. Sohn, Three-dimensional structural displacement estimation by fusing monocular camera and accelerometer using adaptive multi-rate Kalman filter, Engineering Structures, Vol 292 2023